JOURNAL OF MATERIALS SCIENCE 40 (2005) 1327–1331

Effect of the purity of CdTe starting material on the impurity profile in CdTe/CdS solar cell structures

M. EMZIANE*, K. DUROSE
Department of Physics, University of Durham, South Road, Durham, DH1 3LE, UK
E-mail: m.emziane@durham.ac.uk

A. BOSIO, N. ROMEO
INFM, Department of Physics, University of Parma, Parco Area delle Scienze 7a, 43100 Parma, Italy

D. P. HALLIDAY
Department of Physics, University of Durham, South Road, Durham, DH1 3LE, UK

We have investigated CdTe/CdS/In_2O_3:F/glass solar cell structures using quantitative SIMS for profiling the impurity distribution from the CdTe free surface through to the glass substrate. Ion implanted CdTe standards were used. The effect of the purity of the CdTe starting material was determined by studying two structures grown from 7N and 5N source materials. Particular emphasis was placed on the potentially electrically active impurities that may originate from the CdTe starting material, and are likely to affect the CdTe/CdS solar cell performance. It was shown that Cu, Zn, Sn, Sb and Pb profiles had the same level and shape in the CdTe layer regardless of the purity of the starting material used, and were therefore not originating from the starting material. Cl, O, Na and Si showed higher levels for structures grown using 5N purity CdTe compared to those from 7N, and may, at least in part, be due to the CdTe starting material used. It was also postulated that at least some impurities (in addition to Cl) may partially come from the $CdCl_2$ treatment, and/or from the TCO (In) and glass (for Si and Na). Te and S interdiffusion at the CdTe/CdS interface was also shown to be enhanced when 5N CdTe source material is used as compared to 7N.
© *2005 Springer Science + Business Media, Inc.*

1. Introduction

In order to improve the stability and lifetime of CdTe/CdS solar cells, intrinsic material properties as well as external influences need to be addressed. A deep understanding of the relationship between electrically active impurities and device performance is also of great importance for the sake of achieving efficiencies higher than those demonstrated so far. The investigation of the impurities originating from the source materials has received very little interest despite its potentially crucial impact on the performance of polycrystalline thin film solar cells. It was reported [1] that nominally identical cells made from 5N CdTe sources of slightly different purity lead to devices with different grain size, V_{oc}, FF and efficiency. Furthermore, the same study showed that cells fabricated with the less pure starting CdTe have lower doping at the back contact than those made with pure material, as shown by quantum efficiency and C-V measurements [1]. These effects were attributed to impurity compensation and/or grain size though the latter itself is affected by the presence of impurities. It is also well known that the distribution of Cu influences the performance and stability of CdTe/CdS solar cells [2].

Because of its high sensitivity, secondary ion mass spectrometry (SIMS) is one of the most powerful analytical techniques and is used extensively for the characterisation of device structures [3]. A review of SIMS capabilities in investigating thin film solar cells was published recently [4]. A literature survey regarding CdTe-based solar cells shows a noticeable lack of quantitative SIMS analysis on entire device structures through to the glass substrate, and there is no comprehensive study of impurity level and distribution within the structures. Also the effect of the purity of CdTe starting material on the impurity distribution within the structure has not been studied.

Stability aspects in CdTe/CdS solar cells were extensively investigated in recent years by means of qualitative SIMS [5–7] where Cu and/or Cl diffusion into the cell structure for cells back-contacted with Cu-containing material were observed. More recently, it

*Author to whom all correspondence should be addressed.

was shown that a cause of degradation of the cells is the diffusion of back contact materials into the active layer, with the diffused impurities tending to accumulate in CdS and at the front contact CdS/TCO interface [2]. Other qualitative SIMS studies on CdTe based solar cells were also reported [8–12].

Some quantitative analyses on CdTe/CdS structures were reported by Durose *et al*. [1, 13]. They investigated structures in their fresh, light-soaked and bake-tested states where several impurities were depth-profiled [13], and studied the diffusion from Sb-Te back contacts to CdTe in as-deposited as well as air annealed test structures [1]. A more recent quantitative SIMS study of CdTe/CdS/SnO_2:F structures grown by pulsed laser ablation and ion sputtering deposition was published [14]. However, this study used either HgCdTe relative sensitivity factors (RSFs) or a model for the quantification and was restricted to impurities that were mainly due to the adsorption from the residual gas atmosphere during the growth (H, C and O).

In this study, a dynamic and quantitative SIMS analysis was performed to determine the impurity species present together with their distribution and level in CdTe/CdS/In_2O_3:F/glass solar cell structures. Particular emphasis is made on the potentially electrically active impurities present in the CdTe source material, and which are therefore more likely to affect the CdTe/CdS solar device performance.

2. Experimental details

We used two CdTe/CdS solar cell structures that were fabricated using the same process. Two types of starting CdTe material of either 7N (99.99999%) or 5N (99.999%) purity were used in order to distinguish the effect of the starting material purity on the impurity profile in the whole solar cell structure. The 7N CdTe was synthesised directly from the elements under high purity conditions at GEC-Marconi Infra-Red and the 5N material was purchased from Cerac. These structures without contact to CdTe were grown in the University of Parma (Italy). They were deposited on fluorine-doped indium oxide (In_2O_3:F) coated soda lime glass as it was shown that this transparent conducting oxide (TCO) gives the best efficiency for solar cells grown using this process [15]. In_2O_3:F (800 nm thick @ 0.5–1 nm/s) and CdS (150 nm thick @ 1 nm/s) layers were grown by sputtering with a typical substrate temperature of 500 and 200°C respectively at an argon partial pressure of 10^{-3} mbar. The CdTe layer (8–10 μm thick @ 2 μm/min) was deposited using close-space sublimation (CSS) with an argon partial pressure of 1 mbar and a source to substrate distance of about 4 mm. The temperatures were 500°C for the substrate and 650°C for the source. Prior to the CdTe deposition, the CSS chamber was cleaned up by heating the crucible and the substrate holder at 800°C for at least 30 min. Both structures were then heat-treated with $CdCl_2$ at 400°C in air for 30 min and chemically etched with Br_2-methanol for few seconds. The $CdCl_2$ used was the subject of a separate study by a chemical analysis carried out using inductively-coupled plasma mass spectrometry (ICPMS) [16].

A set of ion-implanted standards was depth profiled to determine the relative sensitivity factors (RSFs) of the elements, and these were used to perform quantitative SIMS analysis. Implantation was carried out at room temperature using a 200 keV implanter. Depending on the species implanted, low doses between 1.6×10^{12} and 5×10^{13} cm^{-2} were used to reach a maximum concentration level of 10^{18} cm^{-3} for all the implants. The SIMS standards were undoped CdTe (Japan Energy) single crystals, the implantation being done at the University of Surrey Ion Beam Centre with Cl, O, Cu, Na, In, Sb, Sn, Si, Zn, Pb, and S. The depth profiles were performed at QinetiQ (U.K.) using a CAMECA ims-4f SIMS. The cesium (14.5 keV) and oxygen (8 keV) primary ion beams were used to determine the negative and the positive ion yield, respectively. The size of the raster on the samples was $\sim 60 \times 60$ μm^2 for Cs^+ and $\sim 150 \times 150$ μm^2 for O_2^+. In order to distinguish the effect of the purity of the CdTe source material, depth profiles of ^{208}Pb, ^{28}Si, ^{115}In, ^{37}Cl, ^{23}Na, ^{18}O, ^{63}Cu, ^{121}Sb, ^{64}Zn, ^{121}Sn, ^{34}S and ^{128}Te were recorded for each of the two structures from the CdTe free surface through to the glass substrate and performed twice to confirm repeatability. The CdTe surfaces of the structures investigated in this work were not pre-smoothed, either mechanically or chemically, so as not to introduce extraneous contaminants that may affect the SIMS data. In order to get accurate quantification, the samples were profiled under conditions similar to the standard implants.

3. Results

Fig. 1 shows the quantitative SIMS depth profiles of Zn, Pb, Cu, Sn and Sb for the CdTe/CdS/In_2O_3:F/glass solar cell structures grown using CdTe starting material of 5N (a) and 7N (b) purity. For both purities of the starting material, these impurity elements have essentially a flat and constant level throughout the CdTe layer. The corresponding concentrations in both structures are about 4×10^{18} cm^{-3} for Zn, 2×10^{15} cm^{-3} for Pb, 10^{17} cm^{-3} for Cu, 10^{14} cm^{-3} for Sn and 10^{16} cm^{-3} for Sb. One can notice that in the case of Sb the character of the signal indicates that the detection limit is reached.

For the other layers of the structures (i.e. CdS and TCO), the profiles of Zn and Pb conserve the same level and shape regardless of the purity used for the CdTe starting material. However, comparison of Fig. 1(a) and (b) indicates that Cu, Sb and Sn show higher levels in CdS layer when 5N CdTe is used as compared to 7N.

The quantitative depth profiles of Cl, O, Na and Si in the CdTe/CdS/In_2O_3:F/glass solar cell structures are shown in Fig. 2(a) (5N CdTe) and (b) (7N CdTe). For these four impurity elements, the concentration in the CdTe layer is higher when 5N purity source material is used compared to 7N. The increase in impurity concentration is particularly substantial for Si and O. Si is raised from a plateau at 4×10^{16} cm^{-3} to a maximum of about 3×10^{19} cm^{-3}, while O is raised from around 3×10^{18} cm^{-3} to 2×10^{19} cm^{-3}. For both Si and O impurities alike, the profiles from 7N source material have a quite uniform level in CdTe layer.

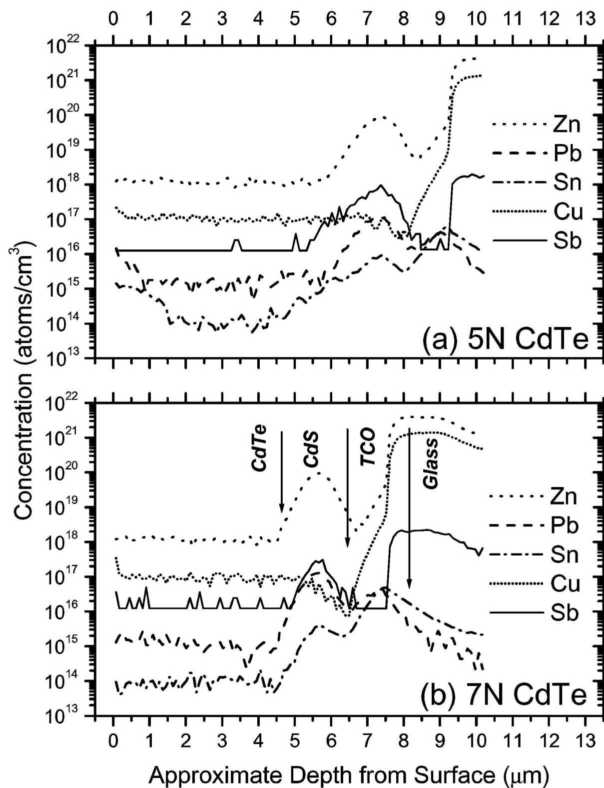

Figure 1 Species in the CdTe layer that are independent of the starting material purity: Quantitative SIMS depth profiles of Zn, Pb, Sn, Cu, and Sb impurity atoms for the CdTe/CdS/In_2O_3:F/glass structures grown using 5N (a) and 7N (b) starting material. The free surface of the CdTe is at depth zero and the approximate positions of the interfaces are shown in Fig. 1(b). While all of the impurities are present at similar levels in the CdTe of both structures, there is an increase in Cu, Sb and Sn in the CdS for the sample made with 5N CdTe.

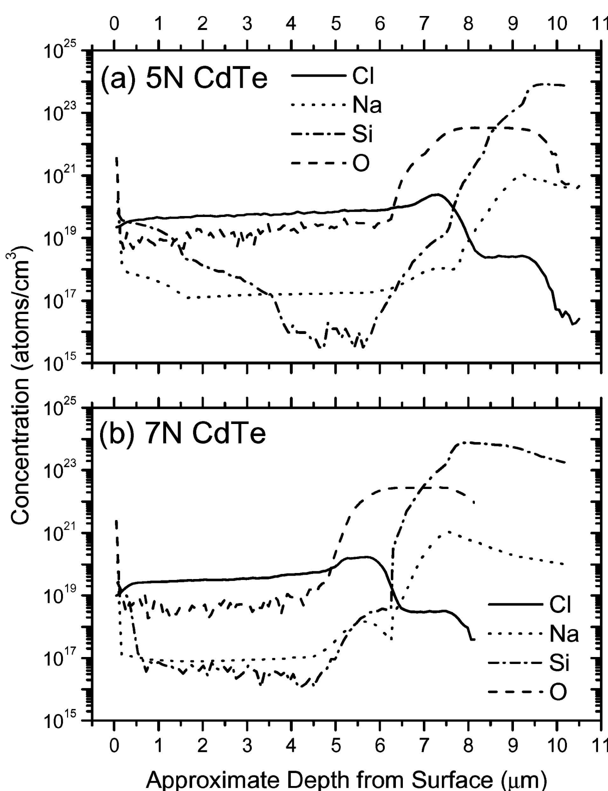

Figure 2 Impurities in the CdTe layer that are probably in part originating from the CdTe starting material: Quantitative SIMS depth profiles of Cl, Na, Si and O impurity atoms for the CdTe/CdS/In_2O_3:F/glass structures grown using 5N (a) and 7N (b) starting material.

For both the 7N and 5N samples the O level in the CdTe is approximately flat, there being a slight rise with depth into the CdTe for the 5N sample. For Si in the CdTe however, there is a more marked difference: while the profile is flat in the 7N sample, there is a marked decrease in the 5N sample, with the highest Si levels appearing as the free surface of the CdTe is approached, and again nearer the glass substrate.

The increase in impurity level in the CdTe active layer is relatively moderate for Cl and Na compared to O and Si, and both Cl and Na depth profiles exhibit a plateau in this layer regardless of the starting material purity used. The changes are from a concentration of about 3×10^{19} to 5×10^{19} cm^{-3} for Cl, and from a level of 8×10^{16} cm^{-3} to nearly 10^{17} cm^{-3} for Na, when 7N and 5N purity were used, respectively. In the CdS layer, however, the levels of Na and O do not seem to change by using 5N or 7N source CdTe but those of Si and Cl increase when 5N purity is used in the growth of CdTe instead of 7N.

Fig. 3 shows the quantitative SIMS depth profiles of S, Te and In for the CdTe/CdS/In_2O_3:F/glass solar cell structures grown using CdTe starting material of 5N and 7N purity. For Te, the concentration is shown on an arbitrary scale rather than cm^{-3}. In this figure, the 7N depth profiles have been shifted forward so that they coincide with and overlap the 5N profiles at the CdTe/CdS interface. This will also make it easier to compare the actual thickness of the CdTe, CdS and In_2O_3:F layers in the 7N structure versus the 5N one. S in CdTe as well as

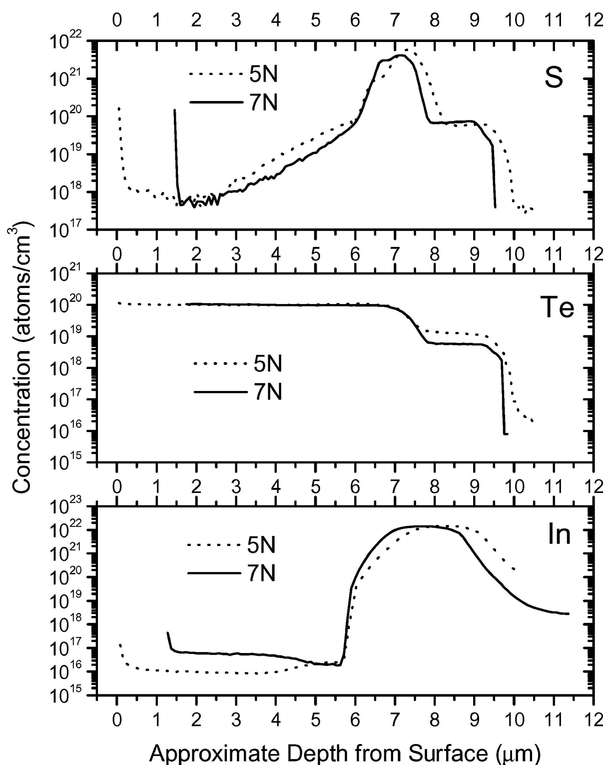

Figure 3 Species from the cell layers: Quantitative SIMS depth profiles of S, Te and In impurity atoms for the CdTe/CdS/In_2O_3:F/glass structures grown using 5N (a) and 7N (b) starting material. Note that for Te the concentration is in arbitrary units (a.u.) instead of cm^{-3}. Note also that the 7N depth profiles have been shifted forward so that they coincide with and overlap the 5N profiles at the CdTe/CdS interface, allowing a thickness comparison for the structure layers.

Te in CdS profiles have slightly higher concentrations in layers for the 5N structure compared to the 7N one. Within the CdTe layer, In depth profiles exhibit a plateau with a concentration of about 6×10^{16} cm^{-3} (for 7N) and about 1×10^{16} cm^{-3} (for 5N). At the CdTe/CdS interface, these profiles cross each other as the In level steadily increases (for 5N) and decreases (for 7N) to reach a flat level and almost the same concentration in the CdS layer for both structures.

4. Discussion

Within the SIMS depth resolution, the CdS and TCO layers under the CdTe appear reasonably well resolved for both structures and the approximate locations of the interfaces (i.e. CdTe/CdS, CdS/TCO and TCO/glass) are clearly apparent in the figures. The depth profiling reached the glass substrate for all the impurity elements investigated except Cl, O, S and Te where it has been stopped at a depth of about 8 μm. The depth scales shown in all the figures are approximate since they were calculated assuming a constant sputter rate that is, in fact, much higher in CdTe than in CdS, TCO and glass, and thus the CdTe thickness is significantly underestimated. The figures also indicate that the actual thickness of the layers is different from the nominal one, and also from one structure to the other. It is particularly interesting to notice that, in the 5N structure, the CdTe layer is at least about 1.7 μm thicker that in the 7N one (see shifts in Fig. 3), and this is mainly due to errors in thickness control at the very high CSS growth rate (2 μm/min) of CdTe.

As mentioned in Section 2, the CdTe free surfaces of the structures studied here were not pre-smoothed so as not to introduce extraneous contaminants that may distort the SIMS analysis. These surfaces appeared rough for both structures and the profiles of some elements like Na, S, O, and Si (7N profile only in the latter) exhibit a surface tailing which mainly results from the CdTe surface roughness and probably also from an increase in crater bottom roughness while sputtering further in depth. Furthermore, the CdTe layer thickness and crystallinity, as well as the roughness of the interfaces are also known to have an effect on the depth resolution.

With this SIMS investigation, we focussed on the impurities coming from the CdTe source material that are crucial to CdTe/CdS solar devices. The aim was to identify those impurities that may come from the CSS source material by using both 7N and 5N feedstock. Such impurities can be expected to act as dopants in the CdTe active layer affecting therefore its physicochemical properties and, ultimately, the CdTe/CdS solar cell characteristics. We will limit our discussion of the quantitative SIMS data from the CdTe layer of the structures, although a qualitative description of the results for the CdS layer is given in the previous section. Fig. 1 shows clearly that Pb, Sn, Zn, Sb and Cu have invariant levels in the CdTe layer for both types of structure (5N and 7N), and suggests therefore that these impurity elements are not originating from the CdTe starting material alone. Te and S interdiffusion at the CdTe/CdS interface was shown to be enhanced slightly when 5N CdTe is used as compared to 7N (Fig. 3). Cl, O, Na and Si (Fig. 2) showed higher levels for structures grown using 5N purity CdTe compared to those from 7N, meaning that, at least in part, these impurity elements are likely to be due to the CdTe starting material used. Alternatively some other aspect of the materials quality (e.g. grain size and diffusion related effects) may be influential in bringing impurities to the CdTe layer in the 5N structure.

It should be emphasised that, except for Sn and Pb, the impurity concentrations recorded in the structure grown with 7N CdTe are well above the total impurity level of 2×10^{15} cm^3 expected in material of this grade. Some of the concentrations (Zn, O, and especially Cl from processing) are even higher than the 2×10^{17} cm^{-3} total that can be anticipated in the case of 5N purity source material. Since both structures have undergone identical preparation steps, we can conclude from this result that at least some of these foreign impurities are mostly incorporated during the post-growth treatment. This comprises $CdCl_2$ heat treatment in air for half an hour at 400°C and Br_2/methanol etching. An ICPMS study of the $CdCl_2$ starting material used in this work is published in [16]. The levels recorded in the powder were Na (5.26 ppm), In (~0.94 ppm) and Sb (0.21 ppm). The presence of high levels of Si in both samples, together with the observed increase in the 5N sample indicate that Si may originate from both impure source material and from some aspect of the growth or processing.

As no trace of Si was detected in the $CdCl_2$ starting material used [16], migration from the glass substrate or incorporation from the reactor environment should be considered. Na may reasonably be expected to originate from the glass substrate and/or from the $CdCl_2$, and that may account for the similarities in the profiles in both structures (Fig. 2). Fig. 3 shows a rather unexpected finding for In, namely that higher levels were recorded in the CdTe of the 7N structure compared to those for the 5N structure. It is unlikely that this excess of In results from the 7N CdTe directly. Instead, we propose that it is from the In_2O_3:F TCO, and that out-diffusion of In into the CdTe is influenced by the thickness of the CdS layer: from the S profiles in Fig. 3(a), it can be seen that the CdS layer in the 7N sample is thinner than that in the 5N structure.

For O, the profiles in the CdTe of both samples are flat, there being a slightly higher level in the 5N sample. This does not show the character of a diffusion profile.

It has recently been shown that CdTe surface composition has a strong effect on the device performance [17]. We therefore note that for the structure deposited using 5N purity, the profiles from the CdTe surface and down to about 1 μm depth show levels around 10 times higher than in the bulk for the cases of Pb and Sn (Fig. 1(a)), Na (Fig. 2(a)) and S (Fig. 3). On the other hand, the structures show an accumulation of In (Fig. 3) as well as an impoverishment of Cl (Fig. 2) near the CdTe surface region regardless of the source material purity used.

The metallurgical junctions in polycrystalline CdTe/CdS solar cells were recently reported to coincide with the electronic junctions [18]. The electronically active layers and interfaces were also investigated and their properties were correlated to the solar cell efficiency [19]. In particular, it was shown that high efficiency cells have usually relatively graded interfaces while cells with low efficiency exhibit abrupt interfaces [19].

In our case, the surface roughness of the structures limited the assessment of interface sharpness by SIMS. It appears, nevertheless, that for both structures the CdTe/CdS active interface is smoother than the CdS/In_2O_3:F interface. More importantly, In, Si, Pb, Zn and Sn depth profiles recorded seem to suggest that the CdTe/CdS interface is slightly graded when 5N purity is used compared to 7N. S and Te profiles, however, show that this interface has the same shape regardless of the purity of the source material used.

5. Conclusions

In conclusion, quantitative and dynamic SIMS measurements were carried out to study the concentration and distribution of impurity elements all the way across CdTe/CdS/In_2O_3:F/glass solar cell structures in order to distinguish the effect of the purity of the CdTe starting material. A set of ion-implanted single crystal CdTe standards was depth profiled for this purpose, and 7N and 5N CdTe source materials were used to grow the CdTe active layer of these structures. It was demonstrated that Cu, Zn, Sn, Sb and Pb had similar profiles in the CdTe layer regardless of the purity of the starting material used, and were therefore not originating from the starting material. Cl, O, Na and Si showed higher levels for structures grown using 5N purity CdTe compared to those from 7N, meaning that, at least in part, these impurity elements are likely to be enhanced as a direct or indirect result of using 5N feedstock. Since most impurities exhibited concentrations much higher than can be expected from the 7N and 5N purity CdTe starting materials used, the impurities must originate from the other cell components or from processing. Some impurities may partially come from the $CdCl_2$ activation process performed in air at 400°C (e.g., Cl itself, Na and Sb), and/or from the TCO (like In) and glass substrates or reactors (for Si and Na). Te and S interdiffusion at the CdTe/CdS interface was also shown to be slightly enhanced when 5N CdTe source material is used as compared to 7N.

Acknowledgements

The authors are thankful to A. J. Pidduck and A. J. Simons (QinetiQ, UK) for SIMS measurements, M. Funaki (Japan Energy) for providing CdTe single crystals, and C. Jeynes and N. Peng (Ion Beam Centre, University of Surrey) for advice on SIMS calibration. They are grateful to Peter Capper (GEC Marconi InfraRed) for supplying the 7N CdTe and would like also to thank the EPSRC for financial support under grant GR/R39283/01.

References

1. K. DUROSE, D. BOYLE, A. ABKEN, C. J. OTTLEY, P. NOLLET, S. DEGRAVE, M. BURGELMAN, R. WENDT, J. BEIER and D. BONNET, *Phys. Stat. Sol.* **229**(2) (2002) 1055.
2. D. L. BATZNER, A. ROMEO, M. TERHEGGEN, M. DOBELI, H. ZOGG and A. N. TIWARI, *Thin Solid Films* **451/452** (2004) 536.
3. K. TSUKAMOTO, S. YOSHIKAWA, F. TOUJOU and M. MORITA, *Appl. Surf. Sci.* **203/204** (2003) 404.
4. K. DUROSE, S. E. ASHER, W. JAEGERMANN, D. LEVI, B. E. McCANDLESS, W. METZGER, H. MOUTINHO, P. D. PAULSON, C. L. PERKINS, J. E. SITES, G. TEETER and M. TERHEGGEN, *Progress in Photovoltaics: Research and Applications* **12** (2004) 177.
5. K. D. DOBSON, I. VISOLY-FISHER, G. HODES and D. CAHEN, *Adv. Mater.* **13** (2001) 1495.
6. *Idem.*, *Solar Energy Mater. Solar Cells* **62** (2000) 295.
7. C. NARAYANSWAMY, T. A. GESSERT and S. E. ASHER, in NCPV Photovoltaics Program Review, AIP Conference Proceedings (1999) Vol. 462, p. 248.
8. T. A. GESSERT, M. J. ROMEO, C. L. PERKINS, S. E. ASHER, R. MATSON, H. MOUTINHO and D. ROSE, *Mat. Res. Soc. Symp. Proc.* **668** (2001) H1.10.1.
9. M. TSUJI, T. ARAMOTO, H. OHYAMA, T. HIBINO and K. OMURA, *J. Cryst. Growth* **214/215** (2000) 1142.
10. R. J. ROSENBERG, R. ZILLIACUS, E. L. LAKOMAA, A. RAUTIAINEN and A. MAKELA, *Fresenius J. Anal. Chem.* **54**(3) (1996) 6.
11. D. KRAFT, A. THISSEN, J. BROETZ, S. FLEGE, M. CAMPO, A. KLEIN and W. JAEGERMANN, *J. Appl. Phys.* **94** (2003) 3589.
12. D. L. BATZNER, A. ROMEO, H. ZOGG, R. WENDT and A. N. TIWARI, *Thin Solid Films* **387** (2001) 151.
13. K. DUROSE, M. A. COUSINS, D. S. BOYLE, J. BEIER and D. BONNET, *ibid.* **403/404** (2002) 396.
14. J. A. GODINES, A. VILLEGAS, YU KUDRIAVTSEV, R. ASOMOZA, A. MORALES-ACEVEDO, A. ESCAMILLA, G. ARRIAGA, H. HERNANDEZ-CONTRERAS, G. CONTRERAS-PUENTE, J. VIDAL, M. CHAVARRIA and R. FRAGOSO-SORIANO, *Semicond. Sci. Techn.* **19** (2004) 213.
15. N. ROMEO, A. BOSIO, V. CANEVARI, M. TERHEGGEN and L. VAILLANT ROCA, *Thin Solid Films* **431/432** (2003) 364.
16. M. EMZIANE, C. J. OTTLEY, K. DUROSE and D. P. HALLIDAY, *J. Phys. D: Appl. Phys.* **37** (2004) 2962.
17. B. E. McCANDLESS, S. S. HEGEDUS, R. W. BIRKMIRE and D. CUNNINGHAM, *Thin Solid Films* **431/432** (2003) 249.
18. I. VISOLY-FISHER, S. R. COHEN, D. CAHEN and C. S. FEREKIDES, *Appl. Phys. Lett.* **83** (2003) 4924.
19. Z. C. FENG, H. C. CHOU, A. ROHATGI, G. K. LIM, A. T. S. WEE and K. L. TAN, *J. Appl. Phys.* **79** (1996) 2151.